IEEE Access
Multidisciplinary ⋮ Rapid Review ⋮ Open Access Journal

Received January 13, 2021, accepted January 22, 2021, date of publication January 27, 2021, date of current version February 18, 2021.

Digital Object Identifier 10.1109/ACCESS.2021.3054990

Basketball Player On-Body Biophysical and Environmental Parameter Monitoring Based on Wireless Sensor Network Integration

IMANOL PICALLO GUEMBE[1], PEIO LOPEZ-ITURRI[1,2], JOSÉ JAVIER ASTRAIN[2,3], ERIK AGUIRRE[1,2], LEYRE AZPILICUETA[4], (Senior Member, IEEE), MIKEL CELAYA-ECHARRI[4], (Graduate Student Member, IEEE), JESÚS VILLADANGOS[2,3], AND FRANCISCO FALCONE[1,2], (Senior Member, IEEE)

[1]Electric, Electronic and Communication Engineering Department, Public University of Navarre, 31006 Pamplona, Spain
[2]Institute of Smart Cities, Public University of Navarre, 31006 Pamplona, Spain
[3]Department of Mathematical Engineering and Computer Science, Public University of Navarre, 31006 Pamplona, Spain
[4]School of Engineering and Sciences, Tecnologico de Monterrey, Monterrey 64849, Mexico

Corresponding author: Francisco Falcone (francisco.falcone@unavarra.es)

This work was supported in part by the Ministerio de Ciencia, Innovación y Universidades, Spain, (MCIU)/Agencia Estatal de Investigación (AEI)/Fondo Europeo de Desarrollo Regional (FEDER)/European Union under Grant RTI2018-095499-B-C31 (IoTrain), and in part by the European Union's Horizon 2020 Research and Innovation Program (Stardust-Holistic and Integrated Urban Model for Smart Cities) under Grant 774094.

ABSTRACT Sport activities have benefited in recent years from the progressive adoption of different technological assets in order to improve individual as well as group training, collect different statistics or enhance the spectator experiences. The progressive adoption of Internet of Things paradigms can also be considered within the scope of sport activities, providing high levels of user interactivity as well as enabling cloud-based data storage and processing. In this work, a system for monitoring biophysical, kinematic and environmental parameters within the development of basketball training is presented. A set of on-body nodes with multiple sensors and wireless body area network capabilities have been designed, implemented and tested under real training conditions during a match. Wireless channel analysis results have been obtained with the aid of in house implemented deterministic 3D ray launching algorithm, providing accurate coverage/capacity estimations in relation with human body consideration in the field as well as in the stadium. Measurement results give relevant information in relation with individual player characteristics as well as with team characteristics, providing a flexible tool to improve training development of basketball.

INDEX TERMS Basketball, 3d ray launching, sport, wireless sensor networks, human body kinematics monitoring.

I. INTRODUCTION

It has been so long since wireless technology was first applied in fields such as security, medicine, education and sport. Precisely it is in this last field where wireless communications are experimenting a great impact by improving the good management of these physical activities. The use of Wireless Sensor Networks (WSN) in sports will help to improve the athlete's performance and monitor their health. This opens a new paradigm that can be called the Internet of Sports Things (IoST), which will aid professional athletes to reach their goals using smart wireless sensors networks, applicable on an individual level as well as in the development of team sport activities. Table 1 presents an overview of different approaches in the application of WSN and technological integration within the scope of sport related activities [1]–[16]. In general, these published research studies help the effectiveness of movements or training performance in different kind of sports.

Basketball was created in 1891, in Springfield, Massachusetts by James Naismith professor in order to provide the possibility to practice an indoor sport during the cold winters. This sport reached an Olympic rank in 1936 under the regulation of the International Basketball

The associate editor coordinating the review of this manuscript and approving it for publication was Xiaofan He.

TABLE 1. WSN in sports.

Ref	Description	Application/Research Purposed
[1]	Silicon gets sporty	Description of how using MEMS (microelectromechanical system) in different sports (tennis, baseball, boxing and soccer) can aid professional athletes to maximize their performance.
[2]	Review on Wearable Technology Sensors Used in Consumer Sport Applications	Review of wearable sensors used in consumer sport applications (not professional sport) for athlete performance and injury monitoring.
[3]	Measurement of Angular Motion in Golf Swing by a Local Sensor at the Grip End of a Golf Club	Angular motion measurement algorithm in a golf swing with the aim of training golf players.
[4]	Time multiplexing-star shape body sensor network for sports applications	Wireless channel reliability and efficiency analysis for the deployment of a Wireless Body Area Network (WBAN) for sports applications.
[5]	Node Position Effect on Link Reliability for Body Centric Wireless Network Running Applications	Analysis of the performance of the wireless link on WBAN for running applications.
[6]	Self-Calibrating Body Sensor Network Based on Periodic Human Movements	Optimized body sensor network for running applications using a central gateway which increases devices' lifetime.
[7]	Accurate Wireless Sensor Localization Technique Based on Hybrid PSO-ANN Algorithm for Indoor and Outdoor Track Cycling	Bicycle-coach distance estimation for indoor and outdoor track cycling using WSNs.
[8]	Coverage and capacity of 28 GHz band in indoor stadiums	Presentation of an empirical wireless channel propagation model at 28 GHz for indoor stadiums considering human blockage loss.
[9]	Volleyball Skill Assessment Using a Single Wearable Micro Inertial Measurement Unit at Wrist	A wireless device based on MEMS motion sensor at the wrist to monitor volleyball spikes performance by machine learning algorithms.
[10]	Human Daily and Sport Activity Recognition Using a Wearable Inertial Sensor Network	The authors describe a wearable inertial sensor network with a machine learning classifier to obtain better accuracy for human daily and sport activity.
[11]	IoT for Next-Generation Racket Sports Training	A wearable sensing device based on MEMS which detects badminton strokes helping players in their training.
[12]	Continuous Athlete Monitoring in Challenging Cycling Environments Using IoT Technologies	An IoT-based platform using bicycles as nodes in a Wireless Personal Area Network (WPAN) for real-time cycling monitoring of multiple riders.
[13]	Sensing and monitoring professional skiers	System based on wearable sensors and video recording used to monitoring professional skiers.
[14]	Development of a Real-Time Vital Data Collection System from Players during a Football Game	The study evaluates the packet success rate and diversity gain.
[15]	SAETA: A Smart Coaching Assistant for Professional Volleyball Training	The smart coaching assistant relies on sensing infrastructure that monitors both players and their environment and produces real-time data.
[16]	Wearable Biometric Performance Measurement System for Combat Sports	Design of a wearable system for measurements of athlete's performance in combat sports. Analyzes athletes' shots, postures, and movements.

Federation (Fédération Internationale de Basket-ball, FIBA), which organizes regular competitions. FIBA was founded in 1932 and includes a membership of two hundred and fifteen national associations, divided into five continental federations (Asia, America, Africa, Europe and Oceania).

Basketball is at the moment one of the most important sport, according to the number of participants and regular competitions. For example, in the United States, the National Basketball Association (NBA) is considered one of the best national basketball competitions. This sport has been very important in the history of sports, providing entertainment and developing the practice with the implementation of new technologies. Basketball is considered a cooperation and opposition sport played by two five members' teams in a court. The main goal of the game is to obtain a higher score than the adversary scoring the other team basket, so that, the team getting the highest score will win the match. According to FIBA rules, the court should be flat and firm with the following dimensions: 28 meters in length by 15 meters wide, measured from the inner edge of the boundary line. There will be two team bench zones clearly marked outside the playing court; each bench will have 14 seats for players and coaches. It will also be a scorer's table for basketball officials, scorers, timekeepers, a shot clock operator and a commissioner.

In basketball, new technologies have contributed to the incorporation of some additional devices that improve both physical resistance and players' health. Other devices, however, limit to give further information about the game, for example, the wireless digital scoreboard, that let spectators know the punctuation or the ball possession scoreboard, which works by Bluetooth technology.

Regarding wave diffusion, the surroundings where a professional basketball match is celebrated are very complex. This is so due to the elevated capacity of people that a basketball stadium is able to afford, getting to 15000 spectators occasionally. In addition, it is important to take into account the effect caused by some necessary elements such as backboards and baskets with folding hoops and further furniture so are benches.

There exist many wireless sensors most of which are embedded within the basketball trainer's sole; for example, the Nike Hiperdunk+ trainers [17] able to measure a basketball player's movements, his speed or the height of his jumps and then retransmit this information through Bluetooth so they can be read on the mobile application developed by Nike. The Catapult company has developed another commercial wearable basketball technology called ClearSky T6 [18], which can measure the biomechanical effects of player

movements during training, mitigating injury risk and using wireless communications such as Bluetooth Low Energy (BLE), Ultra Wide Band (UWB) and Wi-Fi technology. The next sensor-based system called ShotTracker [19] was used for the first time in NCAA Division I men's college basketball at the 2018 hall of fame classic. It delivers statistics and analytics to teams and fans enhancing the experience of the game, using shotTracker-enabled ball and deploying sensor on player and anchors in the rafters to track players and ball location.

Another way to obtain information from the game consists in introducing the sensor inside the ball as it is shown in the patent [20] and the paper [21]. In both, the sensor is used to measure the ball's position and acceleration continuously, obtaining, so, a better shot technique. Sometimes the sensor is placed in the back part of the player's hand [22]; in the case of a possible mistake in the shooting, the device will alert the player. The articles in Table 2 are focus on the measuring and detection of players and the ball position in basketball sport using a WSN [23]–[28]. Regarding the data processing in WSN applications, reference [29] includes a data reduction schema between nodes and the Gateway in order to increase the network lifetime using a hierarchical Least Mean Square adaptive filter. In [30], a data analysis (prediction, compression and recovery) framework is presented with the aim of a significant power saving in the monitoring of clustered WSNs for environmental applications. Reference [31] focuses on the difficulties of node organizations in a wireless network, related to different information delivering such as statistics. The work proposes a net topology in order to reduce routing complexity and to obtain a better ability delivering statistical packages. There are other works based on the tracking of the players taking pictures by different cameras in order to detect the movement of the object according to its position in the area; so that, the IT detects these objects based on the segmentation of the images. There are several papers related to that detection of the objects, such as papers based on the Kinect camera [32], [33] or several cameras [34], [35], researches based on movement models [36] and covariance descriptors [37] and detection of players based on the combination not oriented in pictorial structures [38]. In [39], the results of the radar cross-section of basketball ball measurement is presented in order to design a radar system for tracking and detection of the ball. Others research use these tracking data to improve player's performance [40] applying Big Data analysis techniques to increase teams winning rates [41], [42].

The main goal of this paper is the implementation of biophysical/environmental data gathering and analysis solution, based on on-body platforms with wireless communication capabilities in basketball. It is important to note that the experiments presented in this work employed a limited number of sensors (i.e. temperature, humidity and accelerometers) since the objective of the work is the validation and assessment of the overall performance of the designed whole system. The selected hardware is very easily scalable, and the specific sensors required for an application can be added, making the solution very versatile.

TABLE 2. WSN in basketball.

Ref	Description	Application/Research Purposed
[23]	weSport: Utilizing Wrist-Band Sensing to Detect Player Activities in Basketball Games	A tracking system capable of acquiring basketball statistics, such as the number of shots trials, during a one-on-one game with the Microsoft wristband.
[24]	Team Player Tracking Using Sensors and Signal Strength for Indoor Basketball	Wireless tracking of basketball players for team sports providing information about the player's movements, using accelerometer sensors and Radio Frequency (RF) interference signal positioning techniques.
[25]	Basketball Movements Recognition Using a Wrist Wearable Inertial Measurement Unit	In this paper, the movement data of a basketball player (run, dribble, jump, jump shot…) is captured using an inertial measurement unit, which is worn on the wrist and can help the coach's guidance by analyzing the obtained data via Bluetooth.
[26]	UWB Propagation Measurements and Modelling in Large Indoor Environments	This work presents measurements and a channel modelling for UWB in a basketball court within a sports center. The accurate results could aid the use of this technology for sports applications.
[27]	Wrist MEMS Sensor for Movements Recognition in Ball Games	A basketball gesture recognition system using a wrist MEMS device is presented. The system can detect any shooting attempt and posture movements of the arm. Bluetooth 5.0 technology is used between sensors and mobile devices.
[28]	Gesture Recognition of Basketball Referee Violation Signal by Applying Dynamic Time Warping Algorithm Using a Wearable Device	Wearable device for gesture recognition in order to identify basketball referee violation signals (traveling, 24 seconds, returned to backcourt…). The data is sent via Wi-Fi to be processed using a warping algorithm.
This work	On Body Biophysical/Environmental distributed monitoring for individual/team player analysis	On-body sensors (accelerometers, temperature, humidity) connected via a WSN communication systems provide biophysical/kinematics information for individual/group players. Movement/location data and patterns obtained with remote processing/analysis capabilities.

The first step to design the wireless network required for gathering the information provided by the sensors has been performing an accurate wireless channel analysis. By means of this study, the impact of the environment's morphology in the electromagnetic wave propagation is assessed. Additionally, coverage/capacity estimations have been obtained in order to evaluate system's quality of service performance. The proposed solution can be employed in

general by basketball teams for training sessions. Simulation results as well as validation measurements within the University Pavilion of the Public University of Navarre have been obtained and are presented in this work.

The required technology for the research is Xbee S1 units based on the standard IEEE 802.15.4 (ZigBee), which operates in 2.4 GHz frequency setting up a WSN in the research place. In the first place, simulations will be carried out by using 3D Ray Launching (3D-RL) software developed in house in order to perform accurate wireless channel characterization of the complete basketball scenario. Measurement results for channel characterization as well as individual/team data gathering trials are presented, in order to obtain player movement and biophysical data parameters.

This paper is organized as follows: Section II provides a description of a real basketball scenario. The following section provides the details in relation with the wireless channel estimation methodology, as well as with an overview in the state of the art of related propagation models. Section IV presents the simulation and measurement results obtained from the basketball scenario, whereas Section V describes the results obtained from training sessions with the CBS San Jorge Sanduzelai team. Final remarks and conclusions are presented in Section VI.

FIGURE 1. Real scenario under analysis: Sport pavilion located at the public university of navarre.

II. SCENARIO UNDER ANALYSIS

For the development of this work, a real sports venue has been used in order to obtain both measurements and simulation results. The scenario is a sports pavilion, placed at the Public University of Navarre, in the city of Pamplona. The scenario consists of a court where professional basketball and handball matches are usually played, surrounded by stands. The pavilion has capacity for a maximum of 3000 spectators. In Fig. 1, a panoramic photo of the scenario under analysis is shown. In order to carry out simulations by means of an in-house developed 3D Ray Launching algorithm (3D-RL), a simulation scenario has been created based on the planes of the pavilion. The dimensions of the created scenario, which considers the court as well as the stands for the audience, are 51m (length) $\times$ 47m (width) $\times$ 11m (height) and the dimensions of the field inside the pavilion (i.e., the basketball playing court area) are 28m (length) $\times$ 15m (width), as can be seen in Fig. 2. In the created scenario, the basketball court, the baskets with their support, the stands and the metallic fence in the first row of stands are included. As the measurements were taken with the extensible stands folded, the simulation scenario has been built with the extensible stands folded. The stationary stands are those with blue seats in Fig. 1, which corresponds to the stands depicted in black in Fig. 2. On the other hand, extensible stands are the brown benches just under stationary stands (see Fig. 1), which have not been taken into account within the scenario generated with the 3D-RL, due to the fact that during the measurements the extensible stands were not open.

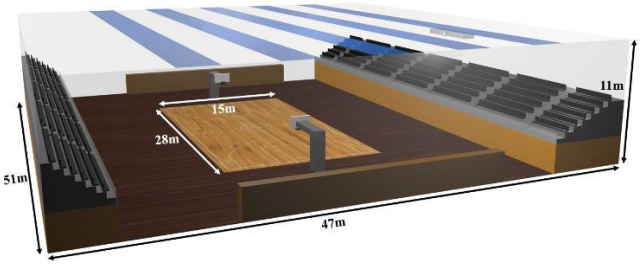

FIGURE 2. Schematic view of the scenario generated for the 3D ray launching simulations.

Regarding the selected technology to carry out this research work, XBee S1 nodes based on the standard IEEE 802.15.4 (ZigBee) have been used. Table 3 presents a comparison of the considered wireless communication technologies. ZigBee is an open global standard for WSN with mesh networking capabilities. The main advantages of the ZigBee protocol are up to 100m of indoor range and the commented mesh support. This makes it a potential candidate for this work since it is necessary to cover around 50m of distance with many potential obstacles within the scenario under analysis (e.g. seats and persons). In addition, the inherent meshing property of ZigBee provides the advantage of reconfiguring the WSN link dynamically, providing high reliability to send the information through the network.

Other communication technologies were considered, such as Bluetooth Low Energy (BLE) and Long-Range Wide Area Network (LoRaWAN), but due to the shorter range of BLE (more appropriate for WBAN networks) and the restrictions on the network topology of LoRaWAN (i.e. no mesh), ZigBee technology was selected to create the WSN. Furthermore, the drawback of employing ZigBee could the higher energy consumption, but due to the short periods of time (during training sessions), this issue is not critical.

III. SIMULATION PROCEDURE

The works presented in Table 1, where different approaches in the application of WSN for sport related activities were shown, do not take into account the effect of fading to RF signals. There are several works in the literature which analyze the effect of fading to RF signals, but these are mostly

TABLE 3. Wireless communication systems.

Wireless Communication System	IEEE 802.15.4 ZigBee Alliance	Bluetooth Low Energy	LoRaWAN LoRa Alliance
Frequency Band	2.4 GHz (ISM) 868 MHz (EU)	2.4 GHz	433, 868 MHz (EU)
Data Rate	250 kbps (ISM) 20 kbps (EU)	1 Mbps	250 bps - 50 kbps
Transmitted Power (max)	10 dBm	20 dBm	14 dBm
Power Consumption	Low/Medium	Very low	Low
Bandwidth	2 MHz	2 MHz	250/125 kHz
Sensitivity	-92 dBm (XBee S1) -100 dBm (XBee-PRO S1)	-70 dBm	-142 dBm
Meshing Capability	Yes	Could be implemented in some devices	No
Range	75-100m (indoor)	10-15m	~3km (urban)
References	https://zigbee alliance.org/	https:/blue tooth.com/	https://lora-alliance.org/

within an office or an indoor environment where significant clutter exists, such as tables, chairs, shelves, cabinets, etc., as well as people movement. Sports environments have certain characteristics that can vary greatly the RF propagation channel, thus showing a behavior significantly different to an office or an indoor environment. Because of that, it is highly important to consider the effects of the specific sport environment in the radio wave propagation channel before the deployment of a wireless communication system. In [43,44], the radio characterization for ISM 2.4GHz WSNs for judo monitoring applications has been presented with the aid of a 3D-RL. Reference [45] presents the characterization of Ultra High Frequency (UHF) radio channels for wireless sensor systems embedded in surfboards. In this work, the channel characterization of a basketball court is presented as an example of a sport environment where players' movement impact is analyzed in terms of signal fading. This specific sport environment has certain characteristics that must be taken into account for the channel characterization, such as the different material properties of the steps in the court, the players' movement or the specific material of the floor and the baskets. It must be pointed out that there is not a big number of clutters in this specific type of sport scenario, in comparison with other indoor environments; however, the presence/movement of the players can considerably affect signal propagation.

It has been reported in the literature that methods based on Ray Tracing (RT) or Geometrical Optics (GO) techniques are the most suitable approaches for the channel characterization for these types of environments, because they achieve a good trade-off between precision results and simulation computational time needed [46]. Because of that, a RT technique, within its version of Ray Launching, has been used in this work for the channel characterization of the specific basketball court environment. The proposed in-house 3D-RL algorithm has been previously validated in different indoor/outdoor sports environments [43]–[45]. The algorithm is based on GO and the Uniform Theory of Diffraction (UTD). The principle of the algorithm is that a certain quantity of rays is launched from the transmitter with a determined angular and spatial resolution. When a ray hits an obstacle, a reflected and refracted ray are created. The reflection coefficient $R^{\parallel\perp}$ and the transmission coefficient $T^{\parallel\perp}$ for the parallel and perpendicular polarization respectively, can be calculated according to the Snell's law [47] by,

$$R^{\parallel} = \frac{E_r^{\parallel}}{E_i^{\parallel}} = \frac{\eta_1 \cos(\psi_i) - \eta_2 \cos(\psi_t)}{\eta_1 \cos(\psi_i) + \eta_2 cos(\psi_t)} \quad (1)$$

$$T^{\parallel} = \frac{E_t^{\parallel}}{E_i^{\parallel}} = \frac{2\eta_2 \cos(\psi_i)}{\eta_1 \cos(\psi_i) + \eta_2 \cos(\psi_t)} \quad (2)$$

$$R^{\perp} = \frac{E_r^{\perp}}{E_i^{\perp}} = \frac{\eta_2 \cos(\psi_i) - \eta_1 \cos(\psi_t)}{\eta_2 \cos(\psi_i) + \eta_1 cos(\psi_t)} \quad (3)$$

$$T^{\perp} = \frac{E_t^{\perp}}{E_i^{\perp}} = \frac{2\eta_2 cos(\psi_i)}{\eta_2 \cos(\psi_i) + \eta_1 cos(\psi_t)} \quad (4)$$

where the sub-index 1 and 2 are referred to two regular different mediums. Then, $\eta_1 = 120\pi/\sqrt{\varepsilon}_{r1}$, $\eta_2 = 120\pi/\sqrt{\varepsilon}_{r2}$, ε_{r1} and ε_{r2} are the relative permittivity of the medium 1 and 2, and ψ_i, ψ_r and ψ_t are the incident, reflected and transmitted angles respectively. $T^{\parallel\perp}$ When a ray hits an edge, a new family of diffracted rays are created. The finite conductivity two-dimensional diffraction coefficients are given by [48], [49] as

$$D^{\parallel\perp} = \frac{-e^{(-j\pi/4)}}{2n\sqrt{2\pi k}} \times \left\{ \begin{array}{l} cot\left(\frac{\pi+(\Phi_2-\Phi_1)}{2n}\right) F\left(kLa^{+}(\Phi_2-\Phi_1)\right) \\ + cot\left(\frac{\pi-(\Phi_2-\Phi_1)}{2n}\right) F\left(kLa^{-}(\Phi_2-\Phi_1)\right) \\ +R_0^{\parallel\perp} cot\left(\frac{\pi-(\Phi_2+\Phi_1)}{2n}\right) F\left(kLa^{-}(\Phi_2+\Phi_1)\right) \\ +R_n^{\parallel\perp} cot\left(\frac{\pi+(\Phi_2+\Phi_1)}{2n}\right) F\left(kLa^{+}(\Phi_2+\Phi_1)\right) \end{array} \right\}$$

where $n\pi$ is the wedge angle, F, L and $a^{\pm}$ are defined in [48], $R_{0,n}$ are the reflection coefficients for the appropriate polarization for the 0 face or n face, respectively. The Φ_2 and Φ_1 angles in would refer to the angles presented in [50].

Once the parameters of transmission T, reflection R, and diffraction D are calculated, the electric field E created by GO and the diffracted electric field created by UTD are calculated by [51],

$$E_{GO}^{\perp\parallel} = \sqrt{\frac{P_{rad} D_t(\theta_t, \emptyset_t)\eta_0}{2\Pi}} \frac{e^{-j\beta_0 r}}{r} X^{\perp\parallel} L^{\perp\parallel} \quad (5)$$

$$E_{UTD}^{\perp\parallel} = e_0 \frac{e^{-jks_1}}{s_1} D^{\perp\parallel} \sqrt{\frac{s_1}{s_2(s_1+s_2)}} e^{-jks_2} \quad (6)$$

where $\beta_0 = 2\pi f_c \sqrt{\varepsilon_0 \mu_0}$, $\varepsilon_0 = 8.854 \cdot 10^{-12}$ F/m, $\mu_0 = 4\pi \cdot 10^{-7}$H/m and $\eta_0 = 120\pi$ ohms. P_{rad} is the radiated power of the transmitter antenna. $D_t(\theta_t, \emptyset_t)$ is the directivity where

rays are launched as defined in the spherical coordinate system at an elevation angle θ_t and an azimuth angle ϕ_t. For each polarization, $X^{\perp\parallel}$ and $L^{\perp\parallel}$ are the polarization ratio and path loss coefficients, r is the distance in the free space and f_c is the transmission frequency. In the diffracted electric field created by UTD, $D^{\perp\parallel}$ are the diffraction coefficients for each polarization, e_0 is the free-space field strength, k is the propagation constant and s_1, s_2 are the distances from the source to the edge and from the edge to the receiver point [50].

The complete scenario is divided in a predetermined three-dimensional mesh by the user and the received power is calculated with the sum of incident electric vector fields in an interval of time Δt inside each cuboid of the defined mesh. All the material properties of all the obstacles within the environment, considering its conductivity and relative permittivity are taken into account, as can be seen in Table 4.

TABLE 4. Material properties for 3D ray launching simulations.

Material	Conductivity (σ) [S/m]	Relative Permittivity (Ɛr)
Aluminum	$37.8 \cdot 10^6$	4.5
Steel	$7.69 \cdot 10^6$	4.5
Nylon	0.24	1.2
Wood	0.21	2.88
PVC	0.12	4
Polypropylene	0.11	3
Glass	0.11	6.06
Concrete	0.02	25
Rubber	$1 \cdot 10^{-14}$	2.61

The developed RL tool provides also the possibility of applying hybrid techniques in order to reduce the computational cost based on the complexity of the analyzed environment. In that sense, the RL algorithm can be hybridized with a Neural Network (NN) module [52], a Diffusion Equation (DE) approach [53], or Collaborative Filtering (CF) module [54], achieving accurate simulation results while computational burden decreases significantly. The employed simulation parameters, complying with convergence criteria, are shown in Table 5.

TABLE 5. Parameter configuration for 3D ray launching simulations.

Parameter	Value
Operation Frequency	2.41 GHz
Transmitted Power	10 dBm
Horizontal angular resolution (ΔΦ)	1º
Vertical angular resolution (Δθ)	1º
Permitted maximum reflections	6
Cuboids size (Mesh resolution)	50cm x 50cm x 50cm
Diffraction phenomenon	Activated

IV. MEASUREMENTS VALIDATION AND SIMULATIONS ANALYSIS

In this section, validation results and simulation analysis with the 3D-RL algorithm are presented. For that purpose, the received power level measurements in the 2.4 GHz band in different areas of interest (basketball court and stands) have been performed. Once the validation is performed, simulations in the form of 2D maps of the RF power level estimations in the case of empty stands are presented, in order to complete radio electrical characterization of the environment. Another key factor to consider is the human presence, so the effect between empty and full stands is analyzed. A priori, it seems clear that larger numbers of people in the stands cause significant attenuation of the received signal, that it could cause worse operation of the devices, so these estimations are necessary for an efficient radio planning of the deployment nodes. The proposed 3D-RL simulation technique enables the consideration of transceiver placement in any location in the scenario, including devices held by users in the audience. In addition, a coverage-capacity analysis has been carried out to evaluate devices' sensitivity requirements.

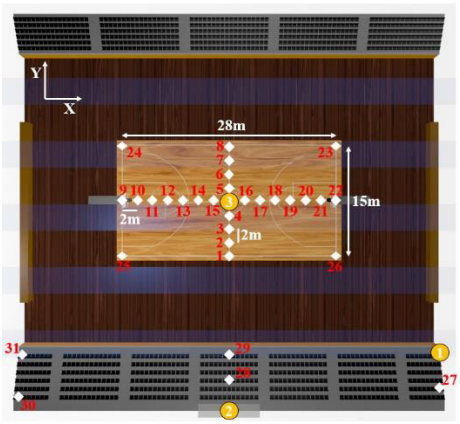

FIGURE 3. Upper view of the created scenario of the pavilion of UPNA. Transmitters and measured points represented by numbered yellow circles and by numbered white diamonds, respectively.

The received power level measurements have been made, placing the transmitter device in three different points (represented by numbered yellow circles) of the basketball pavilion, as shown in Fig. 3. For that purpose, Digi XBee-PRO S1 802.15.4 RF modules have been used, which have been configured with the parameters of Table 5. Transmitter 1 (TX1) is located on a seat at the end of the first row of one of the stands (see Fig. 3 and Fig. 4). Transmitter 2 (TX2) is located in the press zone, where there is a clock (Fig. 5a), and transmitter 3 (TX3) is located at the center of the basketball court, placed on the chest of a man (Fig. 5b) that is looking at the press zone. The received power level has been measured using RF Agilent Fieldfox N9912A analyzer, where the points located at the basketball court (represented by white diamonds numbered from 1 to 26) are 1.20m above the floor, and the points located in the stands (represented by

white diamonds numbered from 27 to 31) are on the seats. Fig. 4 shows the more representative heights of the scenario.

FIGURE 4. Profile view of the scenario that shows the more representative heights.

(a)

(b)

FIGURE 5. Detailed view of transmitters' position: (a) transmitter 2 (TX2) located in the press zone; (b) transmitter 3 (TX3) located at the center of the basketball court, placed on the chest of a man.

In the next figures, validation graphic results are presented, comparing measurements against simulation estimations, performed with the 3D-RL. It should be noted that to simulate the points of TX1 and TX2, the scenario of Fig. 3 has been used with the parameters of Table 5. However, in the case of TX3, the simulation scenario has been reduced to only the basketball court, in order to use 10cm cube resolution on the three axes and in this way, obtain more accurate results. Because of that, for the results of TX3, only the measure points located on the basketball court are presented. In the case of TX1 and TX2, this low resolution is not possible, due to the fact that a divergence effect is produced due to the large dimensions of the scenario and in addition to a significant increment of the computational cost.

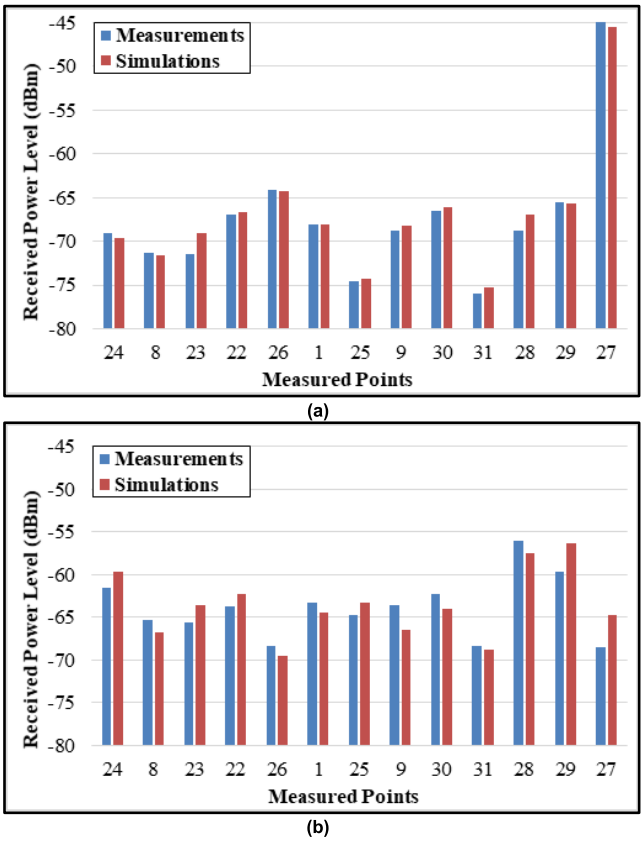

FIGURE 6. Comparison of the measurements and simulations using the 3D-RL: (a) measured points for transmitter 1 (TX1); (b) measured points for transmitter 2 (TX2).

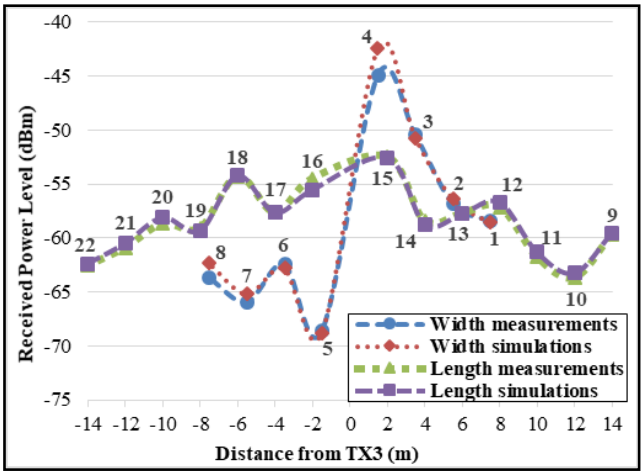

FIGURE 7. Comparison of the measurements and simulations using the 3D-RL for transmitter 3 (TX3), at the width and the height of the basketball court.

Fig. 6 and Fig. 7 show the comparison of the measurements and simulations using the 3D-RL, where the received power level is very similar. In fact, the mean error and the standard deviation of the 48 measured and simulated points are 0.94 dB

and 0.89 dB, respectively. This means that the ray launching simulation model fits the indoor propagation model. It should be noted that TX1 is placed on a seat, which does not have line of sight with many of the measured points in the pavilion, while in the case of TX2 the average received power level for all the measured points is higher because the device is in the high zone of the pavilion. As stated above, each point in Fig. 7 corresponds to the points in Fig. 3 on the basketball court and the TX3 is placed on the chest of a man. It is important to take into account that the man is looking towards the press zone, therefore, as it shows from the points measured at the width of the court (Fig. 7 width measurements), the measured points located behind the human body (5-8 points in Fig. 3) are of lower power. In fact, the 5th point has the lowest power level due to the ''shadow'' effect that the human body produces in the received signal, which is mainly power absorption. For both measurements at the width and length of the court, the behavior of the received power level with the distance clearly shows the multipath propagation, which makes the power level oscillation obtain higher levels in some far points.

Once the simulation algorithm in this large, complex scenario in terms of radio electrical propagation is validated, it is necessary to characterize it completely, deploying nodes at critical points of the scenario and analyzing simulation results. For that purpose, 2D coverage maps are analyzed, between extreme points of the scenario such as the first row and the last row of the stands, or between the basket and the stands, since in addition to the development of a system that helps basketball teams in their training sessions, the idea is to optimize the basketball matches for the fans, who are able to receive statistics in real-time on the smartphone. Furthermore, simulations with people in the stands are presented, to analyze the effect caused in the receiving signal since it could be a limiting factor and make the devices stop working, due to the propagation losses produced by the people.

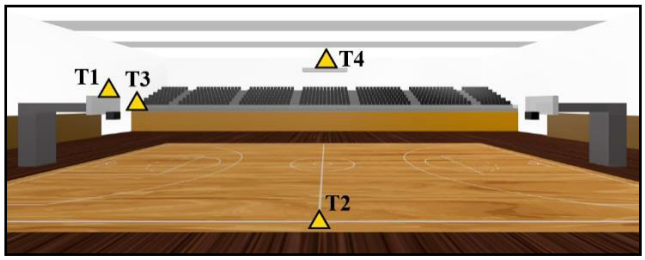

FIGURE 8. Detailed of the transmitters' position (numbered yellow triangles) deployed for simulation analysis: T1 over the basket board, T2 on the court, T3 in the stands and T4 in the press zone.

Following the idea of analyzing the created scenario in terms of range and radio propagation, Fig. 8 shows the transmitters' location (numbered yellow triangles) chosen for simulations. In this way, the most morphologically relevant cases are covered in order to perform an accurate radio planning. The first transmitter (T1) is located over the basket board, which is an interesting point due to its good visibility to cover both the court and the stands, e.g., fans could receive team and players' statistics (points, assists, rebounds, steals…) from this basket during the game in real-time. Another location is to place the transmitter on the field (T2), in this way, the bench zones together with the scorer's table for basketball officials and the players on the court could have coverage. For the transmitter in the stands area (T3), a seat at the end of the first row has been chosen due to its complexity in terms of radio propagation towards other points in the scenario, such as other rows in the stands and certain places on the basketball court. The last transmitter is located in the press zone (T4), where there is a clock at 9.25m height with a line of sight of the whole scenario. It could be a fundamental advantage to place a Wi-Fi access point to cover all wireless devices located in the pavilion.

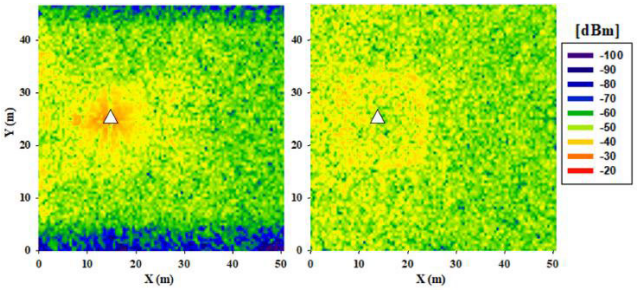

FIGURE 9. Estimated RF power distribution planes for the transmitter T1 located over the basket board (x=14.85m; y=24.98m; z=4m): (a) at the height of the first row of the stand and at the basket height; (b) at the clock height.

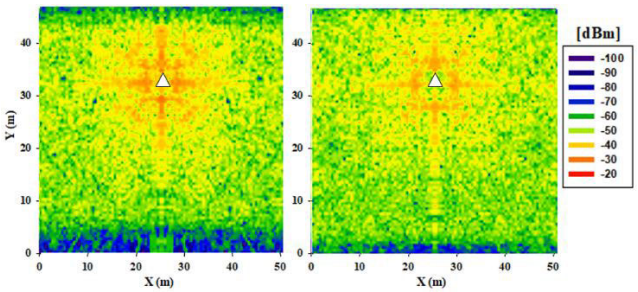

FIGURE 10. Estimated RF power distribution planes for the transmitter T2 on the basket court (x=25.5m; y=32.48m; z=0.1m): (a) at the height of the first row of the stand and at the basket height; (b) at the height of the last row of the stand.

Fig. 9 shows the distributed power estimations in a 2D map at the height of the first row of the stand, at the basket height and the clock height, with the transmitter located over the basket board (heights can be checked in the Fig. 4). In the same way, Fig. 10 shows the distributed power estimations in a 2D map at the height of the first row of the stand, at the basket height and the height of the last row of the stand, with the transmitter located on the basket court. The graph on the left in Fig. 9 shows two areas with a lower power level since there are two areas of stands, one of which is wider because, in reality, the dimensions of the stands are different, as can be seen in Fig. 3.

Fig. 11 depicts the distributed power estimations in a 2D map at the height of the first row of the stand, at the basket height and the clock height, with the transmitter located on

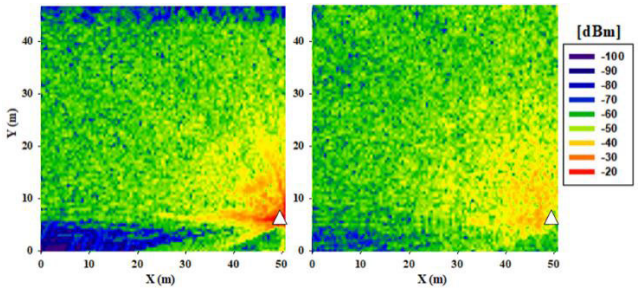

FIGURE 11. Estimated RF power distribution planes for the transmitter T3 located on a seat at the end of the first row of one of the stands (x=50.7m; y=6.15m; z=3.62m): (a) at the height of the first row of the stand and at the basket height; (b) at the clock height.

a seat in the first row of one of the stands. The graph on the left in Fig. 11 shows that having the transmitter in the first row of the stand causes the power level in the back rows to be lower, above all at longer distances from the transmitter. Furthermore, it has been checked that there are acceptable power levels both with the possible devices placed on the baskets and the first row of the other stand. Fig. 12 shows the distributed power estimations in a 2D map at the height of the first row and the height of the last row of the stand, with the transmitter located in the press zone. It can be seen that the people who are not in the stands where the transmitter is located have good coverage due to the unobstructed line of sight.

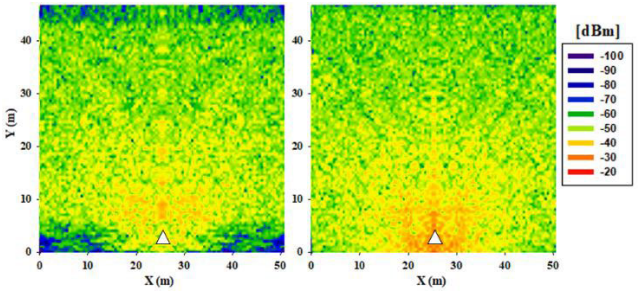

FIGURE 12. Estimated RF power distribution planes for the transmitter T4 located in the press zone (x=25.5m; y=1.45m; z=8.75m): (a) at the height of the first row of the stand and the basket height; (b) at the height of the last row of the stand.

In order to gain insight in relation with volumetric effects, further information can be obtained by representing bi-dimensional vertical planes, in which the complete scenario height is observed, as can be seen in Fig. 13. As expected, higher power levels are detected for the plane nearer to the transmitter (Fig. 13b). All these simulation results show how the morphology of the pavilion plays a key role in the received power level and therefore if the communication between devices is available or not.

Fig. 14 shows one of the stands with the fans, in order to approach by simulation how the human body introduction affects the devices' communication. Fig. 15 depicts the difference in estimated power plane between the simulations with people and without people in the stands, where the transmitter

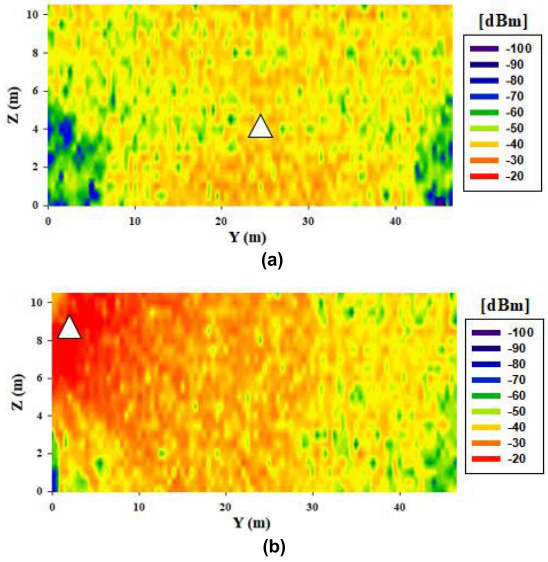

FIGURE 13. Estimated RF power distribution bi-dimensional planes (YZ) corresponding to X-axis = 25.5m: (a) for the transmitter T1 located on the basket court; (b) for the transmitter T4 located in the press zone.

is located on a person sitting in the first row of one of the stands (white triangle). As can be seen, the difference (in dB) is considerable in the stand where the transmitter is located, but also, it is relevant in some zones of the basketball court. Therefore, for efficient radio planning of the wireless system in the pavilion, it is necessary to take people into account.

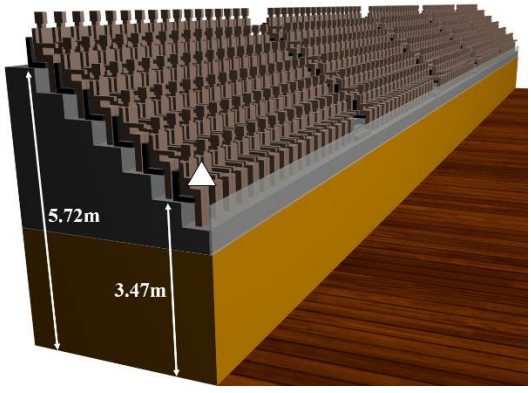

FIGURE 14. Detailed of a full stand including human user body models for simulation analysis.

Finally, a coverage-capacity analysis has been performed in order to assess if the Xbee-PRO S1 devices met with sensitivity requirements (see Table 3). Fig. 16 and 17 show sensitivity planes for the positions of the transmitter in Fig. 9 and 11. As can be seen, for the maximum power transmitted, in both cases, almost all points of the scenario are below the sensitivity level. Although, when the received power level is 0 dBm, there are more points from the court that do not comply with the sensitivity level. It's worth noting that the 3D-RL techniques enables path loss estimation within the complete simulation volume, enabling to obtain optimal node location in order guarantee coverage/capacity relations, as well as to consider elements such as human body

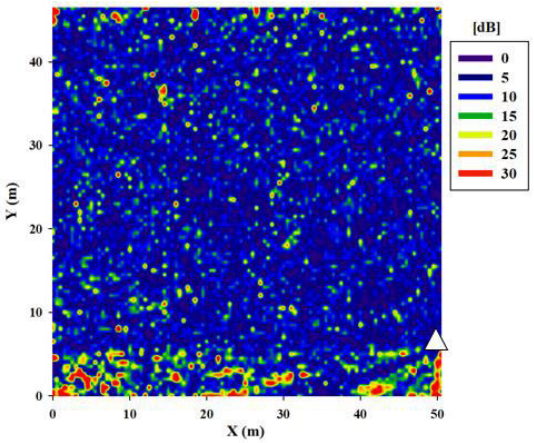

FIGURE 15. Difference in estimated power plane between the simulations with people and without people in the stands, for the transmitter located on a seat/person at the end of the first row of one of the stands (x=50.7m; y=6.15m; z=3.62m).

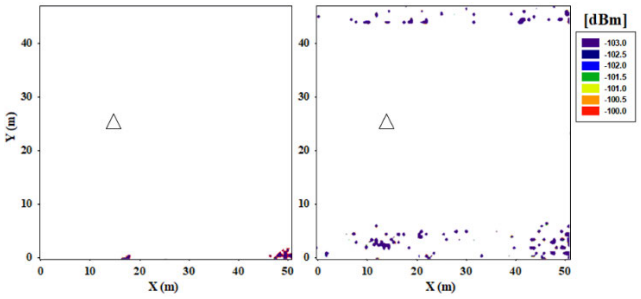

FIGURE 16. Sensitivity planes for the transmitter located over the basket board (x=14.85m; y=24.98m; z=4m) at 1m height for the following transmitted powers: (a) 10 dBm; (b) 0 dBm.

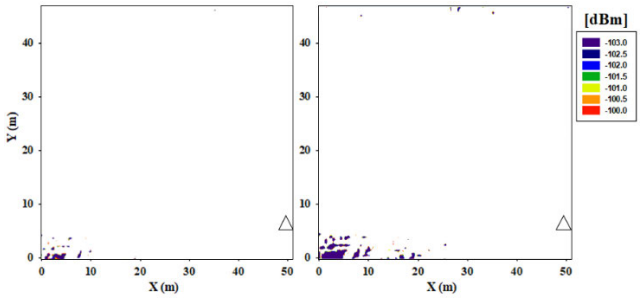

FIGURE 17. Sensitivity planes for the transmitter located on a seat at the end of the first row of one of the stands (x=50.7; y=6.15m; z=3.62m) at the height of the first row of the stand and at the basket height, for the following transmitted powers: (a) 10 dBm; (b) 0 dBm.

shadowing and impact on wireless system performance. The impact of human body motion is mainly given by variations of fast fading, usually modeled by Rice or Rice-K functions. These effects will be considered jointly with precise 3D-RL estimations and human movement channel measurements in future works, including time domain analysis.

V. TRAINING SESSION RESULTS AND ANALYSIS

Once the basketball pavilion has been radio characterized and validated with real measurements, in this section, as another main goal of this work is basketball workout enhancement (technique and strategy), measurements during a real training session of a basketball team are presented. The aim of such study is to assess the validity of the proposed whole system and to test it in a real training situation. In this way, basketball teams will be able to acquire data that could be useful for player health monitoring (implementing the required wearable sensors in the presented solution), as well as improving the tactical and strategy movements at team level, e.g. controlling free spaces in the court in order to execute a more effective attack.

The movements of a basketball team during a match are based on the position of each player on the field. Each position has a specific role, and are as follows (see Fig. 18): Point guard or playmaker, shooting guard, small guard, power forward and center. The playmaker (known as the one), as the best ball handler on the team, focuses on leading and increasing team efficiency. His movements spread out between the area of the three-point line as well as penetrations in the paint. The shooting and the small guard take up the left and the right area in the offensive zone. In the case of the power forward and center, they play with their backs to the basket going in and out of the paint during the game to get the best position to score.

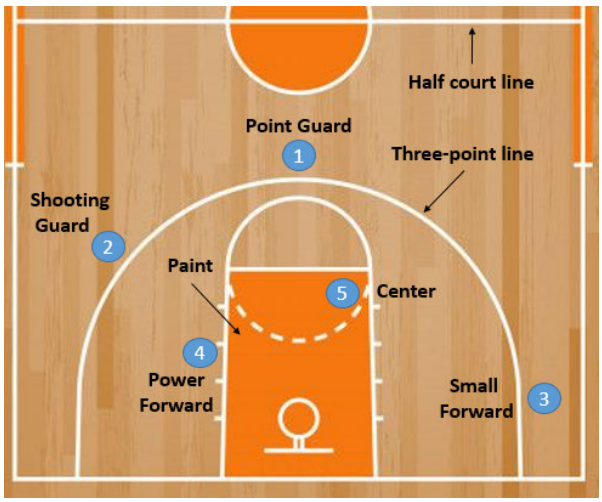

FIGURE 18. Basketball players' position on the court according to their role in the team.

In order to carry out the measurements during the basketball training, XBee S1 802.15.4 RF modules on a Libelium Waspmote V1.1 for each basketball player have been used, which has a three-axis accelerometer integrated among other sensors (temperature, humidity…). The Sensor Nodes have been added to the basketball players' back (lumbar region), and a Gateway node has been placed on the referees' official table for data acquisition. Each node has a Lithium-ion rechargeable battery connected and a vertical monopole antenna of 2.4 GHz (ANT-2.4-CW-RAH) with 1.6 dBi gain. The antenna utilizes a helical element to reduce the antenna's physical length, but this also limits the effective bandwidth allowing an operating range between 2.35-2.6 GHz. Regarding its main characteristics, it has a robust and ultra-compact

design, a right angle mount, omnidirectional radiation pattern and good performance, as well as, low cost. For these reasons, the antenna is ideal for this type of wearable applications, where the reduce size is a key factor.

In order to fix the wireless nodes and sensors on the body of the basketball players, the authors followed the indications and suggestions provided by the amateur basketball players involved in the experiment. Since the accelerometers needed to be attached to the trunk of the human body due to application requirements, the nodes were fixed to the lower back of the basketball players. Thus, the mobility of the players was not hampered and the contact with opponent players was reduced. Additionally, the nodes were packed as seen in Fig. 19b to avoid exposure to sweat. Fig. 19a shows the employed hardware and the Gateway location. Fig. 20 shows several photos taken during the basketball training.

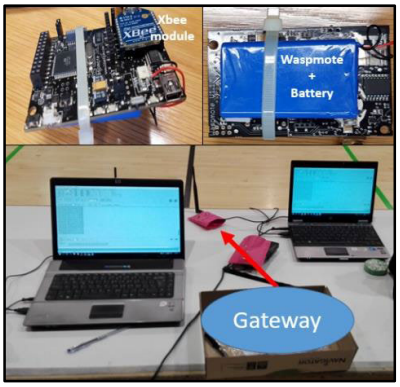

(a)

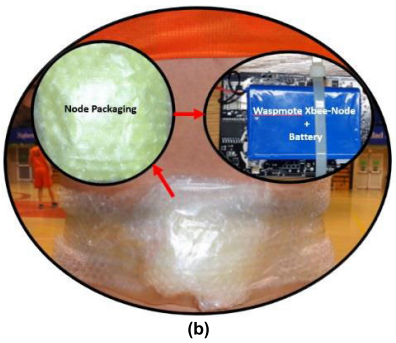

(b)

FIGURE 19. (a) Gateway placed on the referees' official table, and the node's hardware added to the basketball players; (b) Node's packaging on the basketball player's back.

Firstly, as far as communication is concerned, there is a high rate of lost messages (Packet Error Rate, PER), ranging from 28.31% to 80.50%. Although the player's dynamism put the sensors in Non Line of Sight (NLoS) situations, the RSSI values are higher enough to do not lose packets due to the sensitivity of the XBee S1 nodes attached to the players' backs. The obtained high number of lost packets are attributed mainly to the very high data rate (10 packets per second) employed for testing the system, due to collisions and the overflow of packets at the stack of the network coordinator, including the retransmission of the lost packets (ZigBee allows 3 retransmissions per lost packet).

(a)

(b)

FIGURE 20. (a) General view of the court with basketball players on the field; (b) Offensive tactic during the basketball training.

It is important to note that the obtained PER is too high for a reliable network, but the employed data transmission rate was also too high, since we wanted to test the proposed whole system, subjecting the network to a certain stress level. Therefore, although the PER is high, the received packet number is also very high, obtaining enough data to monitor all the basketball players properly.

Regarding the results, shown in Fig. 21, an important deviation in the PER is observed. The rate is acceptable (up to 33%) for the shooting guard (node #2) and small forward (node #3), or even for the center (node #5), but it is very high in the case of the power forward (node #4). In the case of the playmaker (node #1), we observe a high PER value (59.31%), mainly due to its high mobility and its location with respect to that of the gateway. In order to minimize the effect of player movement and location, the system follows a high sending rate (10 packets per second), ensuring enough data harvesting to monitor and analyze player training properly. In this way, data transmission from nodes to the gateway takes place through a best-effort communication, without acknowledgement of message reception. Since the information harvested is not critical at all, and similar information is sent with a high frequency, the implementation of a transport protocol is not appropriate. Fig. 21 summarizes the PER by node. Aggregated PER value shows an average value of 50%, although the deviation is large (28% to 80%).

The RSSI (Received Signal Strength Indicator) values obtained show an average value of -74.27 dBm, and a standard deviation of 5.56 dB. Fig. 22, which includes the RSSI values obtained directly from measurement data provided

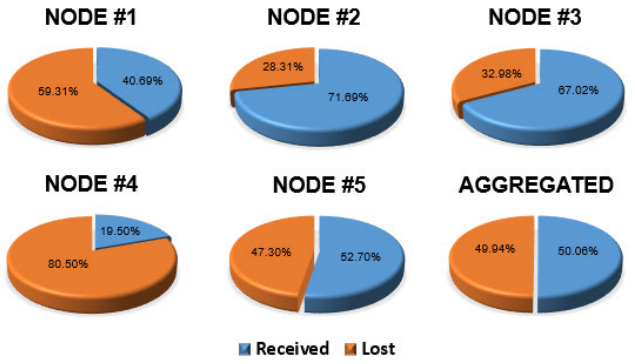

FIGURE 21. Packet error rate by node and aggregated PER.

within the data logs by the ZigBee motes, shows RSSI variations evenly between -60 and -80 dBm for node #5 (Fig. 22a), and that all nodes offer similar values (Fig. 22b). This does not prevent the average RSSI from varying by up to 7 dB between that of node #1 (-72.49 dBm) and node #4 (-79.25 dBm). The medians are respectively -73, -75, -76, -80 and -74 dBm for nodes #1 to #5. The sensitivity of the Xbee S1 802.15.4 devices is up to -92 dBm, as can be seen in Table 3.

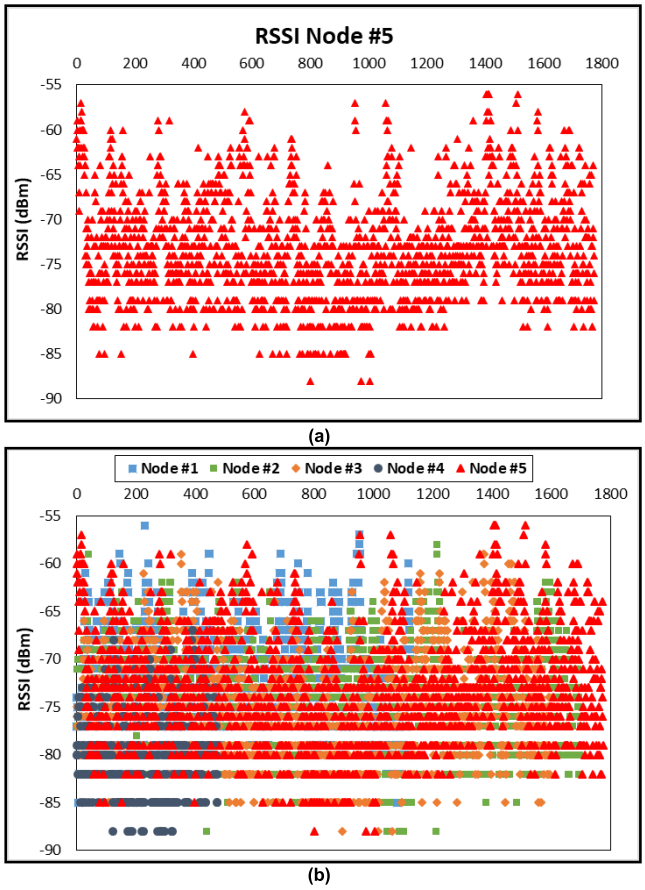

FIGURE 22. (a) Received signal strength for node #5; (b) Aggregated received signal strength by all nodes.

Secondly, as far as training monitoring is concerned, different parameters are measured, such as humidity, temperature

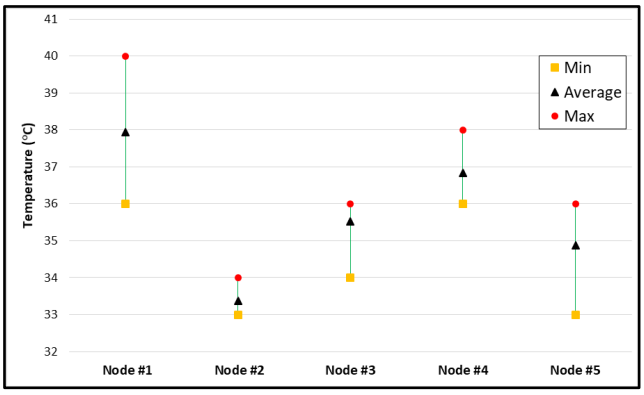

FIGURE 23. Minimum, average and maximum temperature variation of the nodes added on the basketball players.

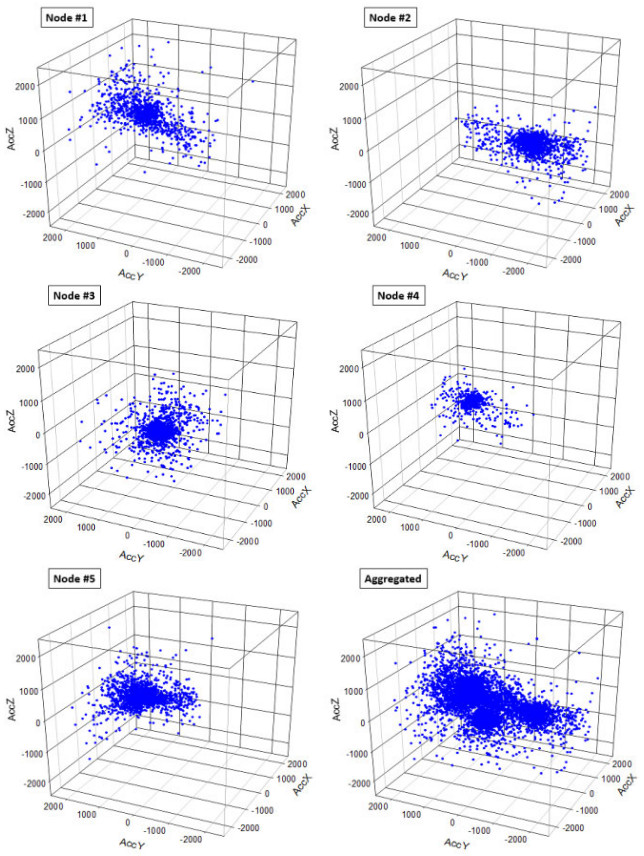

FIGURE 24. Accelerometer data collected from each player and aggregated data collected.

and its variation during training time, movement and displacement of basketball players. Fig. 23 presents the temperature variation of the nodes added to the basketball players' lumbar region. As results shows, some measured values do not correspond to actual body temperatures due to a value of 40°C is not reasonable. It should be noted that for the first prototype of the hardware, the environmental temperature sensor of the Libelium Waspmote has been used in order to emulate a body temperature measurement system. As mentioned before, in order to keep the nodes on the basketball players' body, each node was packed, and in this way, potential injury

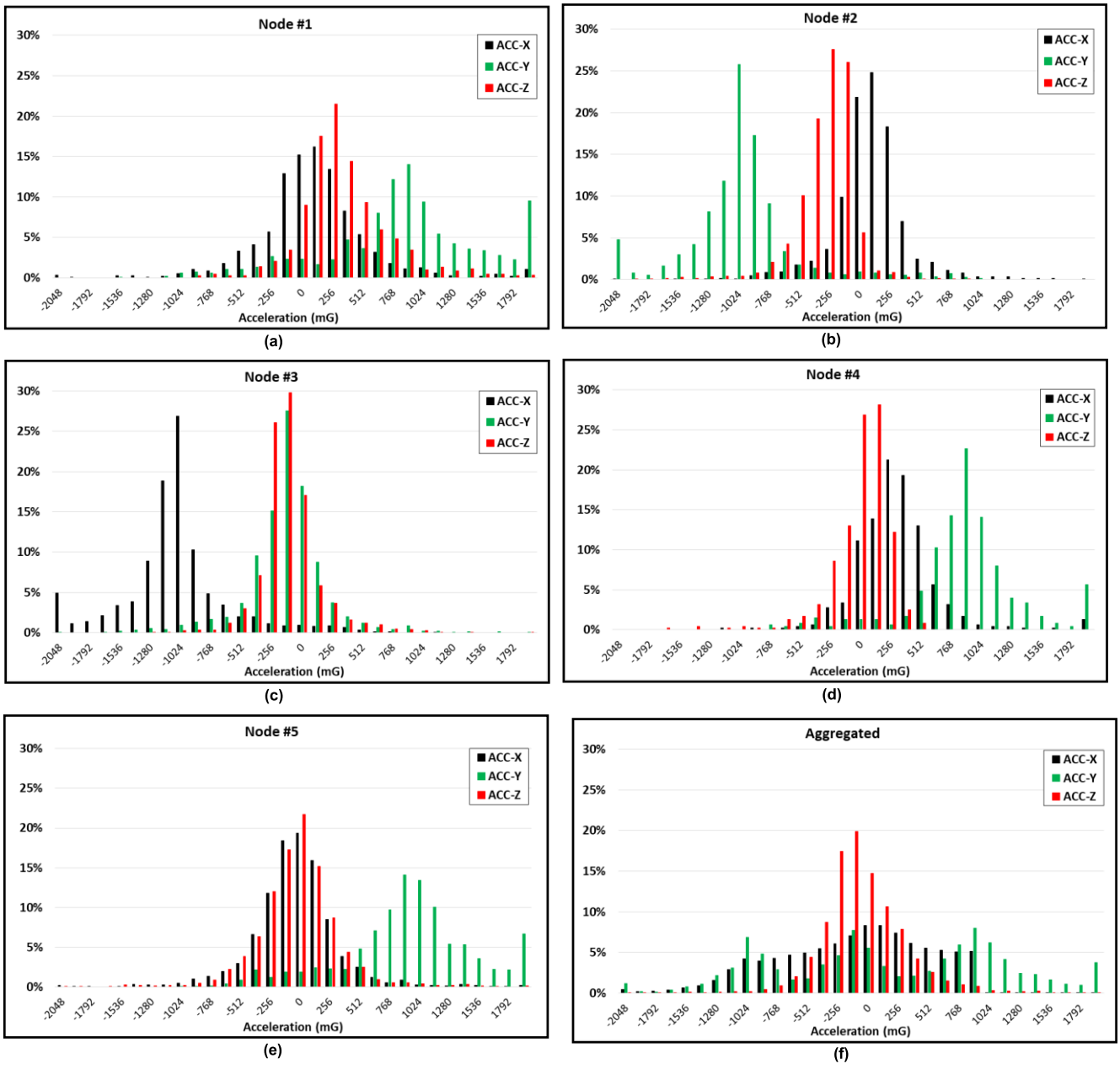

FIGURE 25. Accelerometer data collected distribution from each player: (a) Node #1; (b) Node #2; (c) Node #3; (d) Node #4; (e) Node #5; (f) Aggregated data.

risk was avoided. For these reasons, the packaging of the nodes and its position on the human body could be different for each player due to the movements during training, which could cause these variations on the measured temperature values. However, from the point of view of the data gathering is not critical that some nodes send temperature values out of the expected range.

Thirdly, as far as movement is concerned, Fig. 24 shows the movement readings recorded by the accelerometers that each player carries on his back. Although the sensors can be located in different body positions, they have been chosen to be placed in the lumbar region for ergonomic criteria and to coincide, approximately, with the gravity center. The data analysis shows that some players experience higher acceleration than others do and that the morphology of the movement, and its intensity, differs from one player to another. It can be observed that nodes #1 and #5 are the ones that measure the highest accelerations, which allows us to say objectively that these players are the ones that make the greatest movements. These values show a greater physical effort and a greater active participation of these players.

The highest accelerations in the z-axis correspond to nodes #3 and #5, and the smallest acceleration to node #4. Likewise, node #4 has the least acceleration in the horizontal plane. One can note that this node is the one that offers a greater density of acceleration values, while the dispersion is greater

for the rest of the nodes. Data analysis shows, in this case, that players #1, #3 and #5 are the most mobile, while players #2 and #4 are the least mobile. Player #5 moves on the vertical axis notably more than the rest of the players and practically doubles player #4. Players #1, #3 and #2 are the ones that have more mobility in the horizontal plane (XY).

According to the distribution of probabilities of accelerations, which analyzes the frequency of repetition of these, one can note in Fig. 25 (f) that movement in the horizontal plane (XY) predominates. Flatter curves show greater variability in measured accelerations, implying greater mobility, while curves with a triangular appearance centered on the coordinate origin show greater passivity. The displacement of the curves with respect to the center implies a sustained activity during the time.

How the curves move to one side or the other of the origin is related to the type of movement of the player, and this with the position he occupies on the court. It can be observed again that players #1 and #5 are the ones who move most on the vertical axis, and those players #1, #2 and #4 move more frequently than players #3 and #5 do. This could be due to the fact that the player #1 and #2 are responsible for maintaining defensive balance in attack due to its position on the field (see Fig. 18), and therefore, they have to move more in order to avoid the other team's counter-attack.

VI. CONCLUSION

In this work, a distributed on-body system for the collection and analysis of biophysical and environmental data within the scope of basketball sport development is described. Wireless channel characterization, considering basketball field, pavilion and human body inclusion is performed, by means of deterministic 3D RL simulation code, adapted to the specific requirements of the basketball scenario. An accurate characterization of the entire volume of the scenario has been achieved, obtaining estimated RF power distribution results for different antenna configurations and positions in order to enable interactive communication capabilities. This is applicable for both training sessions and competition matches based on wireless communications, which is useful for player health monitoring, as well as improving the tactical movements at team level. This type of analysis could subsequently lead to the implementation of assistance referee systems and the creation of context-aware environments improving audience satisfaction. However, current FIBA rules do not allow any equipment used by players, which is not included in this official document, so wearables used in this work are not permitted during an official match. As we mentioned in the introduction section, the official rules are being updated continuously to gradually incorporate the technology related to the playing monitoring to basketball sport. As future work, it would be necessary to reduce and improve the devices' encapsulated in order to avoid injuries between players due to basketball is a high contact sport.

The analysis of the data received is mainly of a statistical nature and can be easily automated, so that no major data processing is required and the information can be provided in real time, in order to improve training as well as basketball match development. Future work will focus on the characterization and modeling of time domain parameters as well as on specific data analysis outcomes in training as well as in match sessions.

ACKNOWLEDGMENT

The authors gratefully thank the Public University of Navarre for providing their facilities. They also gratefully thank the kind and patient collaboration of the CBS San Jorge Sanduzelai team.

REFERENCES

[1] K. Lightman, "Silicon gets sporty," *IEEE Spectr.*, vol. 53, no. 3, pp. 48–53, Mar. 2016.
[2] G. Aroganam, N. Manivannan, and D. Harrison, "Review on wearable technology sensors used in consumer sport applications," *Sensors*, vol. 19, no. 9, p. 1983, Apr. 2019.
[3] M. Ueda, H. Negoro, Y. Kurihara, and K. Watanabe, "Measurement of angular motion in golf swing by a local sensor at the grip end of a golf club," *IEEE Trans. Human-Machine Syst.*, vol. 43, no. 4, pp. 398–404, Jul. 2013.
[4] H. A. Sabti and D. V. Thiel, "Time multiplexing-star shape body sensor network for sports applications," in *Proc. IEEE Antennas Propag. Soc. Int. Symp. (APSURSI)*, Memphis, TN, USA, Jul. 2014, pp. 969–970.
[5] H. A. Sabti and D. V. Thiel, "Node position effect on link reliability for body centric wireless network running applications," *IEEE Sensors J.*, vol. 14, no. 8, pp. 2687–2691, Aug. 2014, doi: 10.1109/JSEN.2014.2314477.
[6] H. Abd Ali Sabti and D. V. Thiel, "Self-calibrating body sensor network based on periodic human movements," *IEEE Sensors J.*, vol. 15, no. 3, pp. 1552–1558, Mar. 2015, doi: 10.1109/JSEN.2014.2364586.
[7] S. K. Gharghan, R. Nordin, M. Ismail, and J. A. Ali, "Accurate wireless sensor localization technique based on hybrid PSO-ANN algorithm for indoor and outdoor track cycling," *IEEE Sensors J.*, vol. 16, no. 2, pp. 529–541, Jan. 2016, doi: 10.1109/JSEN.2015.2483745.
[8] M. N. Islam, S. Subramanian, A. Partyka, and A. Sampath, "Coverage and capacity of 28 GHz band in indoor stadiums," in *Proc. IEEE Wireless Commun. Netw. Conf.*, Doha, Qatar, Apr. 2016, pp. 1–7.
[9] Y. Wang, Y. Zhao, R. H. M. Chan, and W. J. Li, "Volleyball skill assessment using a single wearable micro inertial measurement unit at wrist," *IEEE Access*, vol. 6, pp. 13758–13765, Jan. 2018.
[10] Y.-L. Hsu, S.-C. Yang, H.-C. Chang, and H.-C. Lai, "Human daily and sport activity recognition using a wearable inertial sensor network," *IEEE Access*, vol. 6, pp. 31715–31728, May 2018.
[11] Y. Wang, M. Chen, X. Wang, R. H. M. Chan, and W. J. Li, "IoT for next-generation racket sports training," *IEEE Internet Things J.*, vol. 5, no. 6, pp. 4558–4566, Dec. 2018, doi: 10.1109/JIOT.2018.2837347.
[12] E. Municio, G. Daneels, M. De Brouwer, F. Ongenae, F. De Turck, B. Braem, J. Famaey, and S. Latre, "Continuous athlete monitoring in challenging cycling environments using IoT technologies," *IEEE Internet Things J.*, vol. 6, no. 6, pp. 10875–10887, Dec. 2019, doi: 10.1109/JIOT.2019.2942761.
[13] F. Michahelles and B. Schiele, "Sensing and monitoring professional skiers," *IEEE Pervas. Comput.*, vol. 4, no. 3, pp. 40–45, Aug. 2015.
[14] S. Hara, T. Tsujioka, T. Kanda, H. Nakamura, T. Kawabata, K. Watanabe, M. Ise, N. Arime, and H. Okuhata, "Development of a real-time vital data collection system from players during a football game," in *Proc. IEEE 15th Int. Conf. e-Health Netw., Appl. Services (Healthcom)*, Lisbon, Portugal, Oct. 2013, pp. 409–413.
[15] J. Vales-Alonso, D. Chaves-Dieguez, P. Lopez-Matencio, J. J. Alcaraz, F. J. Parrado-Garcia, and F. J. Gonzalez-Castano, "SAETA: A smart coaching assistant for professional volleyball training," *IEEE Trans. Syst., Man, Cybern. Syst.*, vol. 45, no. 8, pp. 1138–1150, Aug. 2015.
[16] S. Saponara, "Wearable biometric performance measurement system for combat sports," *IEEE Trans. Instrum. Meas.*, vol. 66, no. 10, pp. 2545–2555, Oct. 2017.
[17] Nike. (Aug. 12,2012). *Nike Hyperdunk+ 2012*. Accessed: Apr. 27, 2020. [Online]. Available: http://news.nike.com/news/nike-hyperdunk-2012

[18] Catapult. *ClearSky T6*. Accessed: Oct. 2, 2020. [Online]. Available: https://www.catapultsports.com/sports/basketball
[19] ShotTracker. *ShotTracker Technology*. Accessed: Oct. 5, 2020. [Online]. Available: https://shottracker.com/
[20] R. S. Gold, "Intelligent basketball," U.S. Patent 0 325 739, Dec. 31, 2009.
[21] E. Abdelrasoul, I. Mahmoud, P. Stergiou, and L. Katz, "The accuracy of a real time sensor in an instrumented basketball," in *Proc. 7th Asia–Pacific Congr. Sports Technol. (APCST)*, 2015, pp. 202–206.
[22] A. Taniguchi, K. Watanabe, and Y. Kurihara, "Measurement and analyze of jump shoot motion in basketball using a 3-D acceleration and gyroscopic sensor," in *Proc. SICE Annu. Conf. (SICE)*, Akita, Japan, 2012, pp. 361–365.
[23] L. Bai, C. Efstratiou, and C. S. Ang, "WeSport: Utilising wrist-band sensing to detect player activities in basketball games," in *Proc. IEEE Int. Conf. Pervas. Comput. Commun. Workshops (PerCom Workshops)*, Sydney, NSW, Australia, Mar. 2016, pp. 1–6.
[24] J. A. Kirkup, D. D. Rowlands, and D. V. Thiel, "Team player tracking using sensors and signal strength for indoor basketball," *IEEE Sensors J.*, vol. 16, no. 11, pp. 4622–4630, Jun. 2016, doi: 10.1109/JSEN.2016.2542359.
[25] R. Ma, D. Yan, H. Peng, T. Yang, X. Sha, Y. Zhao, and L. Liu, "Basketball movements recognition using a wrist wearable inertial measurement unit," in *Proc. IEEE 1st Int. Conf. Micro/Nano Sensors AI, Healthcare, Robot. (NSENS)*, Shenzhen, China, Dec. 2018, pp. 73–76.
[26] C. Briso, C. Calvo, and Y. Xu, "UWB propagation measurements and modelling in large indoor environments," *IEEE Access*, vol. 7, pp. 41913–41920, Mar. 2019.
[27] X. Zhang, H. Duan, M. Zhang, Y. Zhao, X. Sha, and H. Yu, "Wrist MEMS sensor for movements recognition in ball games," in *Proc. IEEE 9th Annu. Int. Conf. Cyber Technol. Autom., Control, Intell. Syst. (CYBER)*, Suzhou, China, Jul. 2019, pp. 1663–1667.
[28] S. R. Bedico, E. M. L. Lope, E. J. L. Lope, E. B. Lunjas, A. P. D. Lustre, and R. E. Tolentino, "Gesture recognition of basketball referee violation signal by applying dynamic time warping algorithm using a wearable device," in *Proc. 4th Int. Conf. Comput. Methodologies Commun. (ICCMC)*, Erode, India, Mar. 2020, pp. 249–254.
[29] L. Tan and M. Wu, "Data reduction in wireless sensor networks: A hierarchical LMS prediction approach," *IEEE Sensors J.*, vol. 16, no. 6, pp. 1708–1715, Mar. 2016, doi: 10.1109/JSEN.2015.2504106.
[30] M. Wu, L. Tan, and N. Xiong, "Data prediction, compression, and recovery in clustered wireless sensor networks for environmental monitoring applications," *Inf. Sci.*, vol. 329, pp. 800–818, Feb. 2016.
[31] S.-Y. Liew, M.-L. Gan, C. S. Lim, and H. G. Goh, "Basketball net—A flexible and resilient topology for wireless sensor networks," in *Proc. 6th Int. Conf. Ubiquitous Future Netw. (ICUFN)*, Jul. 2014, pp. 87–92.
[32] B. Chen, Z. Huang, W. Yu, Y. Xu, and J. Peng, "Object recognition and localization based on kinect camera in complex environment," in *Proc. IEEE Int. Conf. Robot. Biomimetics (ROBIO)*, Shenzhen, China, Dec. 2013, pp. 668–673.
[33] C.-H. Hsia, C.-H. Chien, H.-W. Hsu, Y.-F. Chang, and J.-S. Chiang, "Analyses of basketball player field goal shooting postures for player motion correction using kinect sensor," in *Proc. Int. Symp. Intell. Signal Process. Commun. Syst. (ISPACS)*, Kuching, Malaysia, Dec. 2014, pp. 222–225.
[34] M. Taj and A. Cavallaro, "Multi-camera track-before-detect," in *Proc. 3rd ACM/IEEE Int. Conf. Distrib. Smart Cameras (ICDSC)*, Como, Italy, Aug. 2009, pp. 1–6.
[35] F. Chen, D. Delannay, and C. De Vleeschouwer, "An autonomous framework to produce and distribute personalized team-sport video summaries: A basketball case study," *IEEE Trans. Multimedia*, vol. 13, no. 6, pp. 1381–1394, Dec. 2011, doi: 10.1109/TMM.2011.2166379.
[36] J. Liu, P. Carr, R. T. Collins, and Y. Liu, "Tracking sports players with context-conditioned motion models," in *Proc. IEEE Conf. Comput. Vis. Pattern Recognit.*, Portland, OR, USA, Jun. 2013, pp. 1830–1837.
[37] L.-S. Wu, L.-M. Xia, Q. Wang, and D.-Y. Luo, "Ball carrier detection and behavior recognition in basketball match using covariance descriptor," in *Proc. Int. Conf. Image Anal. Signal Process.*, Hubei, China, Oct. 2011, pp. 89–93.
[38] Z. Ivankovic, M. Rackovic, and M. Ivkovic, "Automatic player position detection in basketball games," *Multimedia Tools Appl.*, vol. 72, no. 3, pp. 2741–2767, Oct. 2014.
[39] B. Salski, J. Cuper, P. Kopyt, and P. Samczynski, "Radar cross-section of sport balls in 0.8–40-GHz range," *IEEE Sensors J.*, vol. 18, no. 18, pp. 7467–7475, Sep. 2018, doi: 10.1109/JSEN.2018.2862142.
[40] J. Sampaio, T. McGarry, J. Calleja-González, S. Jiménez Sáiz, X. Schelling i del Alcázar, and M. Balciunas, "Exploring game performance in the national basketball association using player tracking data," *PLoS ONE*, vol. 10, no. 7, Jul. 2015, Art. no. e0132894.
[41] Y.-S. Lee, J.-R. Wang, J.-W. Zhan, and J.-M. Zhang, "Data mining analysis of overall team information based on Internet of Things," *IEEE Access*, vol. 8, pp. 41822–41829, Feb. 2020.
[42] S. Shi, Q. F. Zhou, M. Peng, and X. Cheng, "Utilize smart insole to recognize basketball motions," in *Proc. IEEE 4th Int. Conf. Comput. Commun. (ICCC)*, Chengdu, China, Dec. 2018, pp. 1430–1434.
[43] P. Lopez-Iturri, E. Aguirre, L. Azpilicueta, J. Astrain, J. Villadangos, and F. Falcone, "Radio characterization for ISM 2.4 GHz wireless sensor networks for judo monitoring applications," *Sensors*, vol. 14, no. 12, pp. 24004–24028, Dec. 2014.
[44] P. Lopez-Iturri, E. Aguirre, L. Azpilicueta, J. Astrain, J. Villadangos, and F. Falcone, "Implementation and analysis of ISM 2.4 GHz wireless sensor network systems in judo training venues," *Sensors*, vol. 16, no. 8, p. 1247, Aug. 2016.
[45] H. Baghdadi, E. Aguirre, P. Lopez, L. Azpilicueta, J. J. Astrain, J. Villadangos, and F. Falcone, "Characterization of UHF radio channels for wireless sensor systems embedded in surfboards," *IEEE Antennas Wireless Propag. Lett.*, vol. 14, pp. 1526–1529, Mar. 2015.
[46] Z. Yun and M. F. Iskander, "Ray tracing for radio propagation modeling: Principles and applications," *IEEE Access*, vol. 3, pp. 1089–1100, Jul. 2015.
[47] H. D. Hristov, *Fresnel Zones in Wireless Links, Zone Plate Lenses and Antennas*, 1st ed. Norwood, MA, USA: Artech House, 2000.
[48] R. J. Luebbers, "A heuristic UTD slope diffraction coefficient for rough lossy wedges," *IEEE Trans. Antennas Propag.*, vol. 37, no. 2, pp. 206–211, Feb. 1989.
[49] R. J. Luebbers, "Comparison of lossy wedge diffraction coefficients with application to mixed path propagation loss prediction," *IEEE Trans. Antennas Propag.*, vol. 36, no. 7, pp. 1031–1034, Jul. 1988.
[50] L. Azpilicueta, M. Rawat, K. Rawat, F. Ghannouchi, and F. Falcone, "Convergence analysis in deterministic 3D ray launching radio channel estimation in complex environments," *Appl. Comput. Electromagn. Soc. J.*, vol. 29, no. 4, pp. 256–271, 2014.
[51] F. Granda, L. Azpilicueta, M. Celaya-Echarri, P. Lopez-Iturri, C. Vargas-Rosales, and F. Falcone, "Spatial V2X traffic density channel characterization for urban environments," *IEEE Trans. Intell. Transp. Syst.*, early access, Feb. 26, 2020, doi: 10.1109/TITS.2020.2974692.
[52] L. Azpilicueta, M. Rawat, K. Rawat, F. M. Ghannouchi, and F. Falcone, "A ray launching-neural network approach for radio wave propagation analysis in complex indoor environments," *IEEE Trans. Antennas Propag.*, vol. 62, no. 5, pp. 2777–2786, May 2014.
[53] L. Azpilicueta, F. Falcone, and R. Janaswamy, "A hybrid ray launching-diffusion equation approach for propagation prediction in complex indoor environments," *IEEE Antennas Wireless Propag. Lett.*, vol. 16, pp. 214–217, May 2017.
[54] F. Casino, L. Azpilicueta, P. Lopez-Iturri, E. Aguirre, F. Falcone, and A. Solanas, "Optimized wireless channel characterization in large complex environments by hybrid ray launching-collaborative filtering approach," *IEEE Antennas Wireless Propag. Lett.*, vol. 16, pp. 780–783, Aug. 2017.

IMANOL PICALLO GUEMBE received the bachelor's degree in telecommunications engineering from the Public University of Navarre (UPNA), in 2016, and the master's degree in telecommunication engineering from the Charles III University of Madrid (UC3M), in 2019, and the Ph.D. degree in communication engineering from UPNA. He worked with Zener Group Company as a Developer, and is currently working on several public and privately funded research projects. He has more than 15 contributions in indexed international journals and conference contributions. His research interests include radio propagation in inhomogeneous environments, human body interference analysis, wireless sensor networks, the IoT networks, and 5G communications systems. He received the ISSI 2019 Best Paper Award, in 2019, and the Predoctoral Research grant supported by the Government of Navarre, in 2020.

PEIO LOPEZ-ITURRI received the degree in telecommunications engineering, the master's degree in communications, and the Ph.D. degree in communication engineering from the Public University of Navarre (UPNA), Pamplona, Navarre, in 2011, 2012, and 2017, respectively. He gets the 2018 Best Spanish Ph.D. thesis in Smart Cities in CAEPIA 2018 (Third Prize), sponsored by the Spanish network on research for Smart Cities CI-RTI and Sensors (ISSN 1424-8220). He has worked in ten different public and privately funded research projects. In 2019, he partly worked as a Researcher with Tafco Metawireless. He has more than 150 contributions in indexed international journals, book chapters, and conference contributions. He is currently with the Institute for Smart Cities (ISC), UPNA. His research interests include radio propagation, wireless sensor networks, electromagnetic dosimetry, modeling of radio interference sources, mobile radio systems, wireless power transfer, the IoT networks and devices, 5G communication systems, and EMI/EMC. He has been awarded the ECSA 2014 Best Paper Award, the IISA 2015 Best Paper Award, and ISSI 2019 Best Paper Award.

JOSÉ JAVIER ASTRAIN received the degree in telecommunications engineering and the Ph.D. degree in computer science from the Public University of Navarre (UPNA), Spain, in 1999 and 2004, respectively. He has worked in more than 60 different public and privately funded research projects. He works as a Lecturer with UPNA. His current research interests include wireless sensor networks, distributed systems, and cloud computing. He was awarded with the Premio Talgo 2012 for Technological Innovation. He is a coauthor of two Spanish patents. He is a member of the Institute of Smart Cities (UPNA).

ERIK AGUIRRE received the M.Sc. degree in telecommunications engineering from the Public University of Navarre, in 2012, and the Ph.D. degree, in 2014. From 2012 to 2014, he worked in a Research Project with the University of Vigo, related to dispersive propagation. Since 2015, he has been working with Tafco Metawireless. Since 2016, he has been an Assistant Lecturer with UPNA. His research interests include radio propagation in dispersive media, body centric communications, and wireless sensor networks.

LEYRE AZPILICUETA (Senior Member, IEEE) received the degree in telecommunications engineering, the master's degree in communications, and the Ph.D. degree in telecommunication technologies from the Public University of Navarre (UPNA), Spain, in 2009, 2011, and 2015, respectively. In 2010, she worked with the Research and Development Department, RFID Osés, as a Radio Engineer. She is currently working as an Associate Professor and a Researcher with the Tecnologico de Monterrey, Campus Monterrey, Mexico. She has more than 200 contributions in relevant journals and conference publications. Her research interests include radio propagation, mobile radio systems, wireless sensor networks, ray tracing, and channel modeling. She has been recipient of the IEEE Antennas and Propagation Society Doctoral Research Award 2014, the Young Professors and Researchers Santander Universities 2014 Mobility Award, the ECSA 2014 Best Paper Award, the IISA 2015 Best Paper Award, the Best Ph.D. in 2016 awarded by the Colegio Oficial de Ingenieros de Telecomunicación, the N2Women: Rising Stars in Computer Networking and Communications 2018 Award, the ISSI 2019 Best Paper Award, and the Junior Research Raj Mittra Travel Grant 2020.

MIKEL CELAYA-ECHARRI (Graduate Student Member, IEEE) received the degree in computer science engineering and the master's degree in project management from the Public University of Navarre (UPNA), Pamplona, Navarre, in 2011 and 2015, respectively. He is currently pursuing the Ph.D. degree in engineering of science with the Tecnológico de Monterrey, Mexico. He has worked in different research projects at Tafco Metawireless S. L. (telecommunications company placed at Navarre, Spain). He has been Visiting Assistant with the Networks and Telecommunications Research Group, Tecnologico de Monterrey, from 2015 to 2017. His research interests include wireless sensor networks, radiopropagation, dosimetric analysis, project management, and computer science.

JESÚS VILLADANGOS received the bachelor's degree in physics from the University of Basque Country, Spain, in 1991, and the Ph.D. degree in communications engineering from the Public University of Navarre, Pamplona, Spain, in 1999. In 2000, he became an Associate Professor with the Public University of Navarre. He is a coauthor of two Spanish patents. His research interests include distributed algorithms and vehicular networks. He is a member of the Institute of Smart Cities (UPNA). He was awarded with the Premio Talgo 2012 for Technological Innovation.

FRANCISCO FALCONE (Senior Member, IEEE) received the degree in telecommunication engineering and the Ph.D. degree in communication engineering from the Universidad Pública de Navarra (UPNA), Spain, in 1999 and 2005, respectively. From February 1999 to April 2000, he was a Microwave Commissioning Engineer with SiemensItaltel, deploying microwave access systems. From May 2000 to December 2008, he was a Radio Access Engineer with Telefónica Móviles, performing radio network planning and optimization tasks in mobile network deployment. From January 2009 to May 2009, he was a Co-Founding Member and the Director of Tafco Metawireless, a spin-off company from UPNA. He was an Assistant Lecturer with the Electrical and Electronic Engineering Department, UPNA, from February 2003 to May 2009. In June 2009, he become an Associate Professor with the EE Department, being the Department Head, from January 2012 to July 2018, and since July 2019. From January 2018 to May 2018, he was a Visiting Professor with the Kuwait College of Science and Technology, Kuwait. He is currently affiliated with the Institute for Smart Cities (ISC), UPNA, which hosts around 140 researchers, also acting as the Head of the ICT section. His research interests include related to computational electromagnetics applied to analysis of complex electromagnetic scenarios, with a focus on the analysis, design, and implementation of heterogeneous wireless networks to enable context aware environments. He has more than 500 contributions in indexed international journals, book chapters, and conference contributions. He received the CST 2003 and CST 2005 Best Paper Award, the Ph.D. Award from the Colegio Oficial de Ingenieros de Telecomunicación (COIT) in 2006, the Doctoral Award UPNA, 2010, the First Juan Gomez Peñalver Research Award from the Royal Academy of Engineering of Spain in 2010, the XII Talgo Innovation Award in 2012, the IEEE 2014 Best Paper Award, in 2014, the ECSA-3 Best Paper Award, in 2016, and the ECSA-4 Best Paper Award, in 2017.